

Communication

Eco-Friendly Synthesis of Organo-Functionalized Mesoporous Silica for the Condensation Reaction

Surjyakanta Rana ^{1,2,*}, José J. Velázquez ²  and Sreekantha B. Jonnalagadda ^{1,*} 

¹ School of Chemistry and Physics, College of Agriculture, Engineering and Science, University of KwaZulu-Natal, Durban 4000, South Africa

² FunGlass, Alexander Dubček University of Trenčín, Študentská 2, SK-911 50 Trenčín, Slovakia

* Correspondence: surjyakanta.rana@tnuni.sk (S.R.); jonnalagaddas@ukzn.ac.za (S.B.J.)

Abstract: Amine-functionalised mesoporous silica was prepared by the sonication method, a green approach. The method used aminopropyl trimethoxy silane as the amine source and tetraethyl orthosilicate as a silica source. We distinguished its performance compared to the amine-functionalised mesoporous silica sample prepared by the co-condensation method. The sonication method offered better catalytic activity. The amine-functionalised material was fully characterised by different characterisation techniques such as X-ray diffraction, FTIR, CHN, and SEM. The 12.8% of amine-functionalised material (12.A-MCM-41-S) gave excellent selectivity (98%) and conversion (95%). The activity remained almost unchanged for four cycles.

Keywords: mesoporous silica; amine functionalised mesoporous silica; knoevenagel condensation



Citation: Rana, S.; Velázquez, J.J.; Jonnalagadda, S.B. Eco-Friendly Synthesis of Organo-Functionalized Mesoporous Silica for the Condensation Reaction. *Catalysts* **2022**, *12*, 1212. <https://doi.org/10.3390/catal12101212>

Academic Editors: Roman Bulánek and Narendra Kumar

Received: 28 July 2022

Accepted: 1 October 2022

Published: 11 October 2022

Publisher's Note: MDPI stays neutral with regard to jurisdictional claims in published maps and institutional affiliations.



Copyright: © 2022 by the authors. Licensee MDPI, Basel, Switzerland. This article is an open access article distributed under the terms and conditions of the Creative Commons Attribution (CC BY) license (<https://creativecommons.org/licenses/by/4.0/>).

1. Introduction

The porous materials with high specific surface areas are of broader interest, with potential applications in different fields such as gas storage, adsorption, sensor technology, and catalysis [1–8]. Mesoporous silica (M41S) belongs to a family of valuable materials composing MCM-41, MCM-48, MCM-50, and SBA-15, with high surface area, uniform pore size distribution, and easy surface modification potential [9–13]. MCM-41 is unique with accessible surface modification due to the surface silanol groups. The high density of silanol groups on the pore walls facilitates introduction of functional groups with high coverage. The mesoporous silica pores are large enough to accommodate a range of large molecules, such as the organic amine group. Various surface modifications have been introduced to provide new surface functions. The surface modification using amine by the post-synthesis, co-precipitation, and hydrothermal synthesis methods are well documented in the literature [14–18]. Generally, more functional groups on the mesoporous silica improve its catalytic performance. The high density of functional groups on the surface may inhibit molecule transport in the mesopore. The uneven distribution of functional groups in the mesopores negatively impacts the material's performance. For good performance, it is necessary to balance the extensive loading of functional groups with the uniform distribution and the open-pore space. Therefore, we devolved a sonication approach for higher loading of amine compared to the other method and an easy way to apply surface modification.

Several amine-functionalised materials are normally prepared through wet-impregnation and co-precipitation methods for base-catalysed reactions [1,19–25]. Parida et al. reported that amine-functionalised MCM-41 prepared by the co-condensation method gave (92%) conversion and (99%) selectivity, but the post-synthesis method obtained (70%) conversion and (91%) selectivity [26]. The post-synthesis method leads to lower loading of aminopropyl trimethoxy silane (APTES) on the MCM-41 surface than the co-precipitation method. Therefore, they found less activity in the case of the post-synthesis technique. Further, Choudary et al. reported that amine-functionalised mesoporous silica for Knoevenagel

condensation reaction [27]. They prepared diamine-functionalised mesoporous silica by the post-synthesis method. These materials gave 79% conversion and 99% yield in an organic solvent. Wang et al. reported amine-functionalised mesoporous silica by hydrothermal synthesis [28]. His group found 96.8% in both conversion and yield in 12 h. Amino-functionalised mesoporous silica hollow spheres were prepared with the hydrothermal synthesis procedure reported by Wang et al. [29]. They found 100% conversion in the presence of toluene at 4 h. Furthermore, Zhong et al. reported the post-synthesis method's generation of amine-functionalised MCM-41 material. This method yielded 45% conversion and selectivity in 11 h under toluene solvent [30]. We prepared the amine-functionalised mesoporous materials for the first time by the sonication method. For the comparison study, we also prepared 12.8% of amine-functionalised MCM-41 via the co-condensation method [26]. Compared to other reported methods, we achieved better loading, high surface area, and higher catalytic activity with the sonication procedure. Better activity may be due to the higher loading of the amine group on the MCM-41 surface. Further, sonication also encourages the breakdown of hexagonal mesoporous silica agglomerates into more discrete primary particles. That increases the accessible surface to silane.

Here, for the first time, we report the surface modification of amine-functionalised MCM-41 using aminopropyl trimethoxy silane (APTES) by sonication. We also report its catalytic activity toward the Knoevenagel condensation reaction and compare the activity with the material prepared by the co-condensation method.

2. Results

Figure 1a illustrates the FT-IR spectrum of the 12.8-A-MCM-41-S catalyst. The absorption band at 1080–1090 cm^{-1} is the result of the Si-O stretching of the Si-O-Si structure [31]. The bands at 1620–1640 cm^{-1} and 3100–3600 cm^{-1} correspond to H-O-H bending vibration of H_2O and absorption of the water molecule, respectively [32]. In this spectrum, both N-H bending vibration and $-\text{NH}_2$ symmetric bending vibration of amine-functionalised mesoporous silica are represented as 690 cm^{-1} and 1532 cm^{-1} [33]. In addition, CH_2 groups of the propyl chain are characterised by wavenumber at 2935 cm^{-1} . The spectral data confirm the amino functionalisation of the mesoporous silica surface.

Figure 1b illustrates the small-angle X-ray diffraction study of the 12.8-A-MCM-41-S catalyst. As can be seen from Figure 1b, a strong peak at $2\theta = 2.2$ degrees due to (100) plane. Other small peaks indicate the formation of well-ordered mesoporous materials, which follow the higher order of reflections plane for (110), (200), and (210), respectively. All the reflection planes are present within 5 degrees [34]. If we compare 12.8-A-MCM-41-S with MCM-41 [35], a marginal reduction of the (100) peak is observed. The mesoporous nature remains unchanged after modifying the silica network by organic amino groups.

The N_2 - sorption measurement of 12.8-A-MCM-41-S catalyst is shown in Figure 1c. As per the IUPAC nomenclature, [36] the isotherm of the parent MCM-41 material shows an H4-type hysteresis loop with a well-developed step in the relative pressure range ≈ 0.9 . After modification of the organic group in the MCM-41 framework, it seems to lower the P/P0 for the capillary condensation step, showing the shift in pore volume and pore size to a lower value due to the incorporation of the amino group in the pore of the support. The BET surface area of the parent MCM-41 sample was 1380 m^2/g , and a pore volume of 1.28 cm^3/g was reported [37]. With loading the organic amino group, the surface area (985 m^2/g) and pore volume (0.81 cm^3/g) gradually decrease. This decrease may be due to the functionalisation of the substrate inside the mesopores.

Figure 1d illustrates the scanning electron microscopy image of the 12.8-A-MCM-41-S catalyst. As revealed in Figure 1d, the 12.8-A-MCM-41-S catalyst, prepared by the sonication method, shows slightly elliptical morphology with good order. The CHN analysis found 5.52, 1.27, and 1.19 wt.% of C, H, and N, respectively.

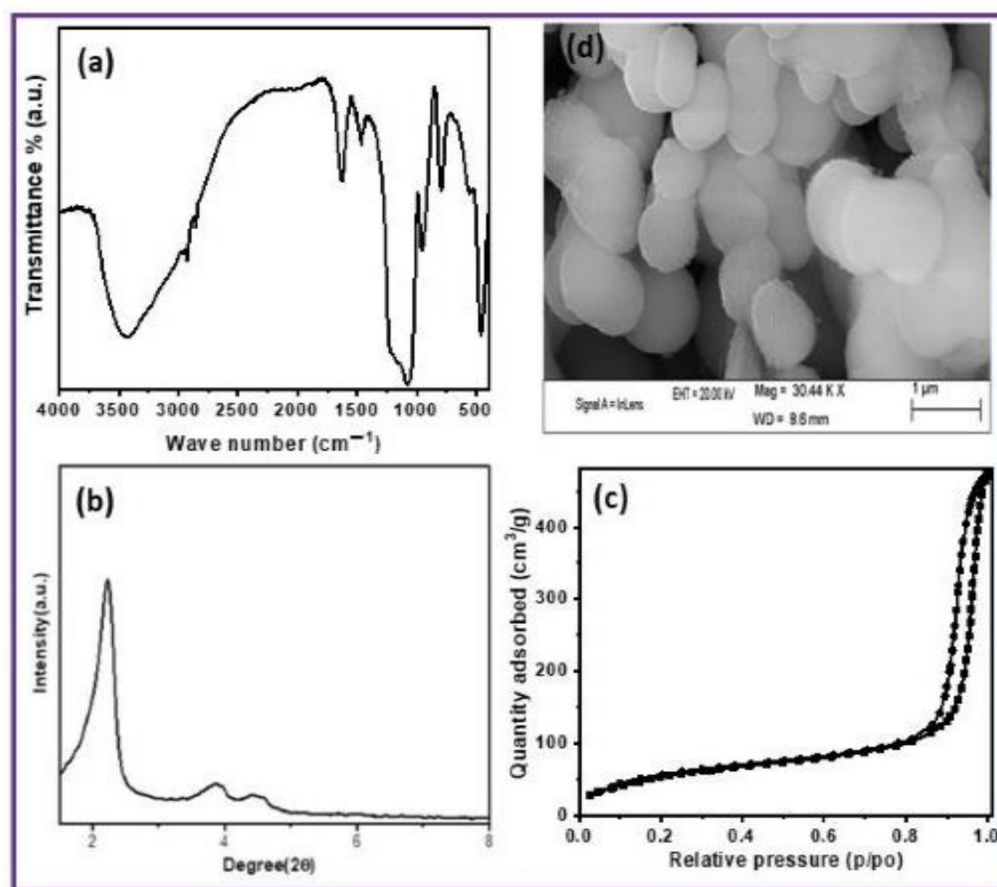


Figure 1. (a) FT-IR spectra, (b) Small-angle XRD pattern, (c) N₂-sorption and (d) SEM image of 12.8-A-MCM-41-S catalyst (Scale bar = 1 μm).

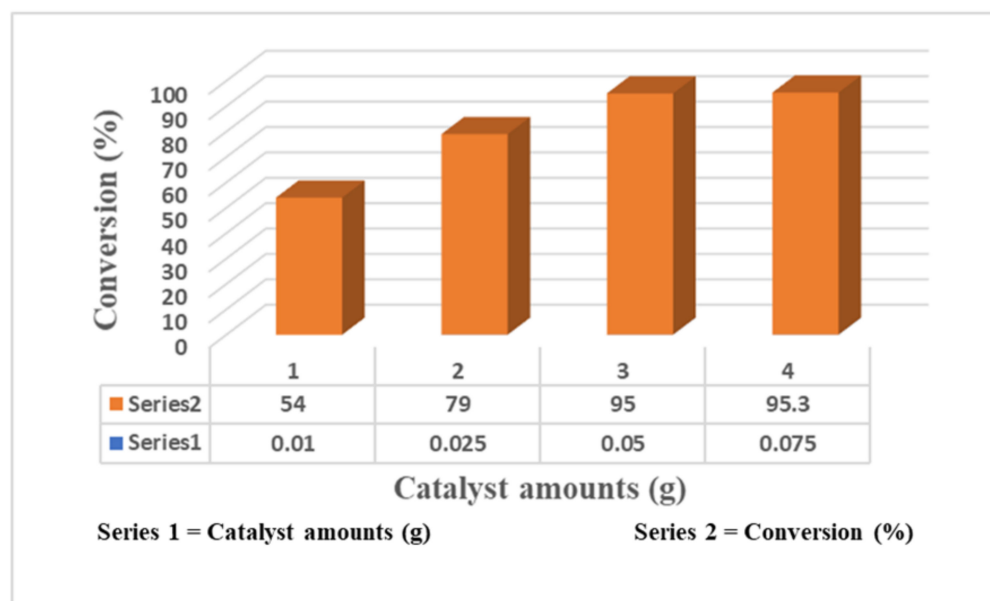
The C-C bond formation reaction between benzaldehyde and diethyl malonate is facilitated by amine-functionalised mesoporous silica. Cinnamic acid is the main product of the Knoevenagel condensation reaction, and Table 1 summarises the results using 12.8-A-MCM-41-S and 12.8-A-MCM-41-C as catalysts for benzaldehyde conversion and selectivity towards cinnamic acid. Our preliminary experiment generated no product without any catalyst at room temperature (RT). The procedure was repeated using parent MCM-41 material at RT, where we saw a 10% conversion, with 51% selectivity towards cinnamic acid. With 12.8-A-MCM-41-S as the catalyst, the % transformation and selectivity were outstanding (95% and 98%, respectively). We employed a 12.8-A-MCM-41-C catalyst for the comparative investigation, made by a co-condensation process. While the selectivity of both catalysts (12.8-A-MCM-41-C and 12.8-A-MCM-41-S) is comparable, the co-condensation catalyst produced roughly 2.6% less conversion. Improved selectivity with 12.8-A-MCM-41-S catalyst may be due to the uniform or higher loading of aminopropyl trimethoxy silane (APTES) on the MCM-41 surface by the sonication than using the traditional stirred reactor technique.

The amount of catalyst for the Knoevenagel condensation reaction under similar conditions was evaluated. The effect of 12.8-A-MCM-41-S catalyst loading on the Knoevenagel condensation reaction is illustrated in Figure 2. An examination of Figure 2 shows that conversion increases from 54 to 95%, increasing the catalyst from 0.01 g to 0.05 g. Then, the conversion marginally increases (only 0.3%), further increasing the catalyst amount.

Table 1. Catalytic activity towards Knoevenagel condensation reaction *.

Sl. No.	Catalyst	Conversion (%)	Selectivity (%)	
			Cinnamic Acid	Other
1	Without catalyst	0	0	0
2	MCM-41	10	51	49
3	12.8 A-MCM-41-S	95	98	2
4	12.8 A-MCM-41-C	92.4	98	2

* Benzaldehyde = 10 mmol, Malonic ester = 10 mmol, Catalyst = 0.05 g, Temperature = RT and Reaction time = 10 h.

**Figure 2.** Variation of catalyst amounts of 12.8-A-MCM-41-S catalyst over Knoevenagel condensation reaction.

The catalytic activities of the different substituents of aldehydes with the malonic ester (fixed) in the presence of 12.8-A-MCM-41-S catalyst are summarised in Table 2. Table 2 shows that all the aldehydes with different electron-withdrawing and donating substituents gave good to excellent yields with 12.8-A-MCM-41-S with lower reaction time. Specifically, the aldehyde substrates with electron donation groups (-CH₃, -OCH₃, -NH₂, etc.) and -NH₂ group in the para position gave better conversion (84%) and selectivity (92%) towards cinnamic acid. The aldehydes with electron-withdrawing (nitro and halo group) substituents and halo substituents showed higher conversion (92%) and selectivity (93%). The results may be due to the enrichment of carbanion at carbonyl carbon of the electron-withdrawing groups than the electron-donating groups.

Table 3 compares the efficacy of several literature-reported materials for the Knoevenagel condensation reaction. The data reveals that % conversion in the current investigation is higher at room temperature. As seen in Table 3, catalysts obtained using the sonication method gave better conversion than classical surface modification. The improved activity may be due to the better loading of functional groups with uniform distribution.

Under controlled circumstances, the 12.8-A-MCM-41-S catalyst was used in recycling tests for the Knoevenagel condensation reaction. After the initial cycle, the catalyst was recovered through filtration, washed with ethanol, and dried at 60 °C. The recovered catalyst was reused, and we continued recycling the material up to five times. Figure 3 illustrates the catalytic activity of the reused catalyst in consecutive cycles. Figure 3 shows

that conversion efficiency (11%) decreases after the 4th cycle. The lowered efficiency may be due to catalyst poisoning by organic impurities.

Table 2. Knoevenagel condensation of aldehyde substituents with diethyl malonate over 12.8-A-MCM-41-S catalyst.

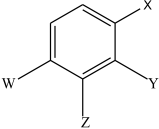
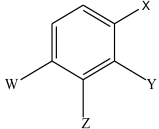
Sl. No.	 Reactant	 Major Product	Conversion (%)	Selectivity (%)	
				Major	Others
1	X = CHO	X = CH = CH-COOH	95	98	2
2	X = CHO, W = NH ₂	X = CH = CH-COOH, W = NH ₂	84	92	8
3	X = CHO, Z = OH	X = CH = CH-COOH, Z = OH	89	91	9
4	X = CHO, W = CH ₃	X = CH = CH-COOH, W = CH ₃	77	85	15
5	X = CHO, Y = OH	X = CH = CH-COOH, Y = OH	85	89	11
6	X = CHO, W = F	X = CH = CH-COOH, W = F	92	93	7
7	X = CHO, W = NO ₂	X = CH = CH-COOH, W = NO ₂	99	99	1
8	X = CHO, W = COH ₃	X = CH = CH-COOH, W = COH ₃	79	83	17
9	X = CH = CH-CHO	X = CH = CH-CH = CH-COOH	97	98	2

Table 3. Effectiveness of the current work in comparison to reported literature.

Catalyst	Temp (°C)	Conversion	Ref.
Amine functionalised MCM-41	RT	92	[26]
Amine-functionalized MCM-41	RT	81	[38]
Aminopropyl-functionalised MCMs	82	84	[39]
12.8-A-MCM-41-S	RT	95	Current work

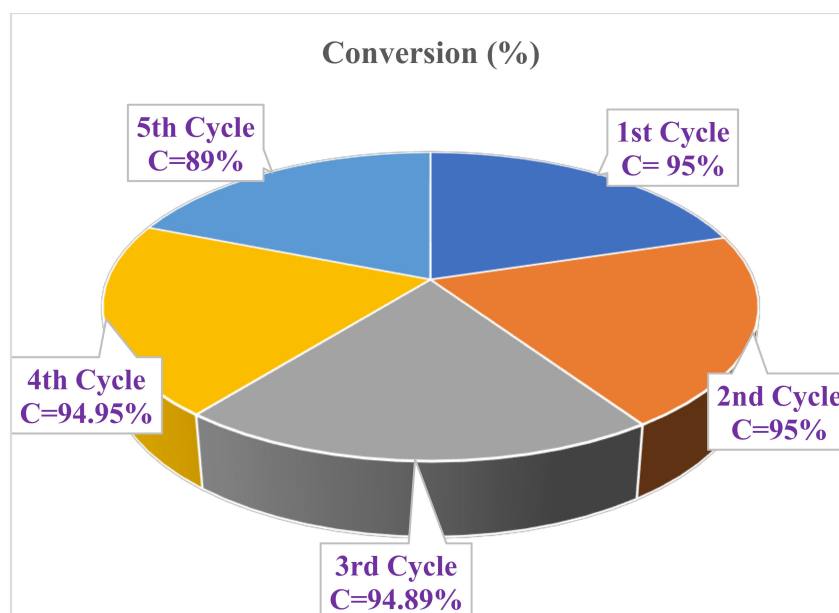


Figure 3. Recycle experiments of 12.8-A-MCM-41-S catalyst.

Figure 4 represents the XRD pattern of the reused catalyst after the fourth cycle. This image demonstrates that the 12.8 A-MCM-41-S catalyst retained its well-defined ordered mesoporous structure.

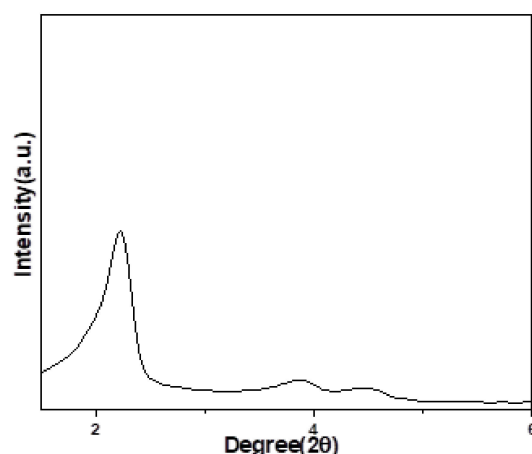
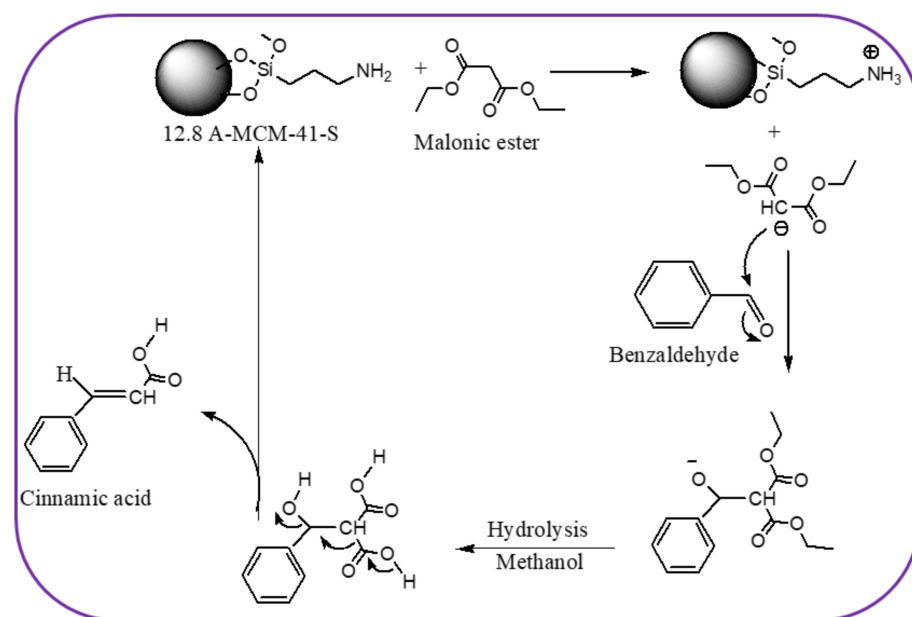


Figure 4. XRD spectrum of the reused catalyst after the fourth cycle.

Scheme 1 depicts the probable mechanism of the Knoevenagel condensation process over 12.8 A-MCM-41-S catalysts. The amino group removes the proton from the diethyl malonate generating the diethyl malonate anion. Following the hydrolysis of the intermediate in the solvent phase, the diethyl malonate anion interacts with the carbonyl carbon of the modified aldehyde to produce the main product, cinnamic acid.



Scheme 1. Mechanism of the Knoevenagel condensation reaction over 12.8 A-MCM-41-S catalyst.

3. Materials and Methods

3.1. Catalysts Preparation

Cetyltrimethylammonium bromide (CTAB, 0.5 g), 2 M of aqueous NaOH (7 mL, 14 mmol), and H₂O (26.67 mmol) are kept in a conical flask and heated at 80 °C for 30 min. The mixture was maintained at a constant pH of 12.4. Then, tetraethyl ortho silicate (TEOS, 9.34 g, 44.8 mmol) and APTES (1.34) mL were added sequentially and rapidly. Following the addition, white precipitation was observed after 3 min. The reaction mixture was sonicated at 60 °C for 4 h. The products were isolated by a hot filtration, washed with a sufficient amount of water followed by methanol, and dried under a vacuum. To remove surfactant, we used 1 g of sample with a mixture of the con. HCl (1) mL and ethanol (100) mL sonicate at 60 °C for 8 h. Then, the mixture was washed with ethanol and dried at 100 °C overnight. Then, the final sample was designated as 12.8 A-MCM-41-S. For comparison, we

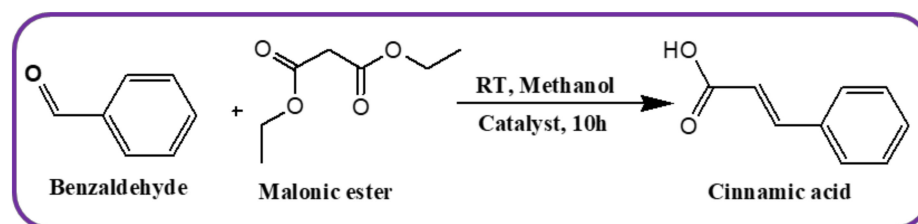
also prepared 12.8% of amine-functionalised mesoporous silica by co-condensation. The sample was designed as 12.8 A-MCM-41-C.

3.2. Catalyst Characterisation

The catalyst's surface area and pore size distribution were determined by N₂ adsorption-desorption at 77 K using the ASAP 2020 (Micrometrics Instruments Corporation, Norcross, GA, USA) instrument. Varian FTIR-800 (Varian Instruments, Randolph, MA, USA) in KBr matrix in the range of 4000–400 cm⁻¹ to record the FT-IR spectra. We used the Thermo Scientific LECO CHNS-932 elemental analyser (Winsford, UK) to obtain the elemental data. The powder X-ray diffraction patterns of the sample were measured by Rigaku D/Max III VC diffractometer (Rigaku, Tokyo, Japan) with Cu K α radiation at 40 kV and 40 mA in the range of $2\theta = 0$ –10 degrees. The FE-SEM was performed with a ZEISS 55 microscope (Carl Zeiss, Oberkochen, Germany).

3.3. Catalytic Activity

Initially, 10 mmol of benzaldehyde, 10 mmol of malonic ester, and 0.05 g of catalyst were taken in the reactor and stirred at room temperature in an oil bath. After 10 h of reaction, 50 mL of methanol was added to soluble all the organic compounds. Then, the mixture was stirred for 10 min (Scheme 2). The catalyst was recovered by centrifugation, and offline GC analysed the reaction mixture.



Scheme 2. Schematic presentation of Knoevenagel condensation reaction.

4. Conclusions

In conclusion, we describe the sonication method's advantage in synthesising organo-functionalized mesoporous material. An XRD and BET surface area revealed that the amino functionalisation material retained mesoporous characteristics. FTIR spectra confirmed the amino attachment onto the MCM-41. The reused materials included the ordered mesoporous structure after the fourth cycle. The 12.8 A-MCM-41-S material may be recycled up to four times and is stable, recyclable, and excellent for the Knoevenagel condensation reaction.

Author Contributions: Conceptualization, formal analysis, initial draft preparation, S.R.; conceptualization, investigation, J.J.V.; resources, methodology, writing—review and editing, supervision, S.B.J. All authors have read and agreed to the published version of the manuscript.

Funding: This research was funded by the University of KwaZulu-Natal (Funding Number: VC22) and also FunGlass (Grant agreement No 739566).

Institutional Review Board Statement: Not applicable.

Informed Consent Statement: Not applicable.

Data Availability Statement: Data is contained within the article.

Acknowledgments: The authors acknowledge the support received from the (i) School of Chemistry & Physics and College of Agriculture, Engineering & Science, University of KwaZulu-Natal, Durban, South Africa, (ii) This work is also a part of the dissemination activities of the FunGlass project. This project has received funding from the European Union Horizon 2020 research and innovation program under grant agreement No 739566.

Conflicts of Interest: The authors declare no conflict of interest.

References

1. Erigoni, A.; Diaz, U. Porous Silica-Based Organic-Inorganic Hybrid Catalysts: A Review. *Catalysts* **2021**, *11*, 79. [[CrossRef](#)]
2. Casco, M.E.; Martínez-Escandell, M.; Gadea-Ramos, E.; Kaneko, K.; Silvestre-Albero, J.; Rodríguez-Reinoso, F. High-Pressure Methane Storage in Porous Materials: Are Carbon Materials in the Pole Position? *Chem. Mater.* **2015**, *27*, 959–964. [[CrossRef](#)]
3. Brotschie, A. Porous materials: MOFs go fungal. *Nat. Rev. Mater.* **2016**, *1*, 15015. [[CrossRef](#)]
4. Li, H.; Li, L.; Lin, R.; Zhou, W.; Zhang, Z.; Xiang, S.; Chen, B. Porous metal-organic frameworks for gas storage and separation: Status and challenges. *Energy Chem.* **2019**, *1*, 100006. [[CrossRef](#)]
5. Furukawa, H.; Ko, N.; Go, Y.B.; Aratani, N.; Choi, S.B.; Choi, E.; Yazaydin, A.Ö.; Snurr, R.Q.; O’Keeffe, M.; Kim, J. Ultrahigh porosity in metal-organic frameworks. *Science* **2010**, *329*, 424–428. [[CrossRef](#)]
6. Salama, R.S.; El-Bahy, S.M.; Mannaa, M.A. Sulfamic acid supported on mesoporous MCM-41 as a novel, efficient and reusable heterogeneous solid acid catalyst for synthesis of xanthene, dihydropyrimidinone and coumarin derivatives. *Colloids Surf. A Physicochem. Eng. Asp.* **2021**, *628*, 127261. [[CrossRef](#)]
7. El-Hakam, S.A.; ALShorifi, F.T.; Salama, R.S.; Gamal, S.; El-Yazeeda, W.S.A.; Ibrahim, A.A.; Ahmed, A.I. Application of nanostructured mesoporous silica/bismuth vanadate composite catalysts for the degradation of methylene blue and brilliant green. *J. Mater. Res. Technol.* **2022**, *18*, 1963–1976. [[CrossRef](#)]
8. Ibrahim, A.A.; Salama, R.S.; El-Hakam, S.A.; Khder, A.S.; Ahmed, A.I. Synthesis of 12-tungestophosphoric acid supported on Zr/MCM-41 composite with excellent heterogeneous catalyst and promising adsorbent of methylene blue. *Colloids Surf. A Physicochem. Eng. Asp.* **2021**, *631*, 127753. [[CrossRef](#)]
9. Hoffmann, F.; Cornelius, M.; Morell, J.; Fröba, M. Silica-Based Mesoporous Organic-Inorganic Hybrid Materials. *Angew. Chem. Int. Ed.* **2006**, *45*, 3216–3251. [[CrossRef](#)] [[PubMed](#)]
10. Rath, D.; Rana, S.; Parida, K.M. Organic amine-functionalized silica-based mesoporous materials: An update of syntheses and catalytic applications. *RSC Adv.* **2014**, *4*, 57111. [[CrossRef](#)]
11. Parida, K.; Rana, S.; Mallick, S.; Rath, D. Cesium salts of heteropoly acid immobilised mesoporous silica: An efficient catalyst for acylation of anisole. *J. Colloid Interface Sci.* **2010**, *350*, 132–139. [[CrossRef](#)] [[PubMed](#)]
12. Rana, S.; Mallick, S.; Mohapatra, L.; Varadwaj, G.B.B.; Parida, K. A facile method for synthesis of Keggin-type cesium salt of iron substituted lacunary phosphotungstate supported on MCM-41 and study of its extraordinary catalytic activity. *Catalysis Today* **2012**, *198*, 52–58. [[CrossRef](#)]
13. Nale, D.B.; Rana, S.; Parida, K.; Bhanage, B.M. Amine functionalized MCM-41: An efficient heterogeneous recyclable catalyst for the synthesis of quinazoline-2, 4 (1 H, 3 H)-diones from carbon dioxide and 2-aminobenzonitriles in water. *Catal. Sci. Technol.* **2014**, *4*, 1608–1614. [[CrossRef](#)]
14. Lim, M.H.; Stein, A. Comparative Studies of Grafting and Direct Syntheses of Inorganic–Organic Hybrid Mesoporous Materials. *Chem. Mater.* **1999**, *11*, 3285–3295. [[CrossRef](#)]
15. Bourlinos, A.B.; Karakostas, T.; Petridis, D. “Side Chain” Modification of MCM-41 Silica through the Exchange of the Surfactant Template with Charged Functionalized Organosiloxanes: An Efficient Route to Valuable Reconstructed MCM-41 Derivatives. *J. Phys. Chem. B* **2003**, *107*, 920–925. [[CrossRef](#)]
16. Brunel, D.; Blanc, A.C.; Garrone, E.; Onida, B.; Rocchia, M.; Nagy, J.B.; Macquarrie, D.J. Spectroscopic studies on aminopropyl-containing micelle templated silicas. Comparison of grafted and co-condensation routes. *Stud. Surf. Sci. Catal.* **2002**, *142*, 1395–1402.
17. Liao, Q.; Zeng, L.; Li, L.; Guo, F.; Wu, L.; Le, S. Synthesis of functionalised mesoporous silica and its application for Cu(II) removal. *Desalin. Water Treat.* **2014**, *56*, 2154–2159. [[CrossRef](#)]
18. Atoub, N.; Amiri, A.; Badiel, A.; Ghasemi, J.B. One-Pot Hydrothermal Synthesis of Functionalized Mesoporous Silica for Effective Removal of Pb(II) Ion. *J. Nanostruct.* **2021**, *11*, 125–135.
19. Yang, Y.; Yao, H.F.; Xi, F.G.; Gao, E.Q. Amino-functionalized Zr(IV) metal-organic framework as bifunctional acid-base catalyst for Knoevenagel condensation. *J. Mol. Catal. A Chem.* **2014**, *390*, 198–205. [[CrossRef](#)]
20. Ren, Y.; Lu, J.; Jiang, O.; Cheng, X.; Chen, J. Amine-grafted on lanthanide metal-organic frameworks: Three solid base catalysts for Knoevenagel condensation reaction. *Chin. J. Catal.* **2015**, *36*, 1949–1956. [[CrossRef](#)]
21. Varadwaj, G.B.; Rana, S.; Parida, K.M. Amine functionalised K10 montmorillonite: A solid acid-base catalyst for the Knoevenagel condensation reaction. *Dalton Trans.* **2013**, *42*, 5122–5129. [[CrossRef](#)]
22. Rana, S.; Jonnalagadda, S.B. Synthesis and characterisation of amine-functionalised graphene oxide and scope as catalyst for Knoevenagel condensation reaction. *Catal. Commun.* **2017**, *92*, 31–34. [[CrossRef](#)]
23. Wang, X.G.; Lin, K.S.K.; Chan, J.C.C.; Cheng, S.F. Direct Synthesis and Catalytic Applications of Ordered Large Pore Aminopropyl-Functionalized SBA-15 Mesoporous Materials. *J. Phys. Chem. B* **2005**, *109*, 1763–1769. [[CrossRef](#)]
24. Suzuki, T.M.; Nakamura, T.; Fukumoto, K.; Yamamoto, M.; Akimoto, Y.; Akimoto, Y.; Yano, K. Direct synthesis of amino functionalised monodispersed mesoporous silica spheres and their catalytic activity for nitroaldol condensation. *J. Mol. Catal. A Chem.* **2008**, *280*, 224–232. [[CrossRef](#)]
25. Neogi, S.; Sharma, M.K.; Bharadwaj, P.K. Knoevenagel condensation and cyanosilylation reactions catalysed by a MOF containing coordinatively unsaturated Zn(II) centers. *J. Mol. Catal. A Chem.* **2009**, *299*, 1–4. [[CrossRef](#)]
26. Parida, K.M.; Rath, D. Amine functionalised MCM-41: An active and reusable catalyst for Knoevenagel condensation reaction. *J. Mol. Catal. A Chem.* **2009**, *310*, 93–100. [[CrossRef](#)]

27. Choudary, B.M.; Kantam, M.L.; Sreekanth, P.; Bandopadhyay, T.; Figueras, F.; Tuel, A. Knoevenagel and aldol condensations catalysed by a new diamino-functionalised mesoporous material. *J. Mol. Catal. A Chem.* **1999**, *142*, 361–365. [[CrossRef](#)]
28. Wang, K.; Jiang, H.; Tong, M.; Xiao, Y.; Li, H.; Zhang, F. Primary amine-functionalised mesoporous phenolic resin as an effective and stable solid base catalyst for Knoevenagel reactions in water. *Green Synth. Catal.* **2020**, *1*, 79–82. [[CrossRef](#)]
29. Wang, H.; Liu, X.; Saliy, O.; Hu, W.; Wang, J. Robust Amino-Functionalized Mesoporous Silica Hollow Spheres Templated by CO₂ Bubbles. *Molecules* **2022**, *27*, 53. [[CrossRef](#)]
30. Zhong, L.W.; Su, B.; Guo, Y.J.; Chu, L.P. Preparation and synergetic catalytic effects of amino-functionalised MCM-41 catalysts. *Sci. China Chem.* **2012**, *55*, 1167–1174.
31. Mikhail, D.; Stepanenko, Y.; Dzenis, Y.; Karotki, A.; Rebane, A.; Taylor, P.N.; Anderson, H.L. Extremely Strong Near-IR Two-Photon Absorption in Conjugated Porphyrin Dimers: Quantitative Description with Three-Essential-States Model. *J. Phys. Chem. B* **2005**, *109*, 7223–7236.
32. Ebrahimi-Gatkash, M.; Younesi, H.; Shahbazi, A.; Heidari, A. Amino-functionalized mesoporous MCM-41 silica as an efficient adsorbent for water treatment: Batch and fixed-bed column adsorption of the nitrate anion. *Appl. Water Sci.* **2017**, *7*, 1887–1901. [[CrossRef](#)]
33. Rahimi, Z.; Zinatizadeh, A.A.; Zinadini, S.; van Loosdrecht, M.; Younesi, H. A new anti-fouling polysulphone nanofiltration membrane blended by amine-functionalised MCM-41 for post treating waste stabilisation pond's effluent. *J. Environ. Manag.* **2021**, *290*, 112649. [[CrossRef](#)] [[PubMed](#)]
34. Matei, C.; Buhălțeanu, L.; Berger, D.; Mitran, R. Functionalized mesoporous silica as matrix for shape-stabilised phase change materials. *Int. J. Heat Mass Transf.* **2019**, *144*, 118699. [[CrossRef](#)]
35. Rana, S.; Mallick, S.; Parida, K.M. Selective oxidation of benzaldehyde by molecular oxygen over molybdovanadophosphoric acid supported MCM-41. *J. Porous Mater.* **2012**, *19*, 397–404. [[CrossRef](#)]
36. Lowell, S.; Shields, J.E.; Thomas, M.A.; Thommes, M. *Characterization of Porous Solids and Powders: Surface Area, Pore Size and Density*; Springer: Dordrecht, The Netherlands, 2006.
37. Rath, D.; Rana, S.; Parida, K.M. Cu_xH_{3-2x}PW₁₂O₄₀ Supported on MCM-41: Their Activity to Heck Vinylation of Aryl Halides. *Ind. Eng. Chem. Res.* **2010**, *49*, 8942–8948. [[CrossRef](#)]
38. Kubota, Y.; Nishizaki, Y.; Ikeya, H.; Saeki, M.; Hida, T.; Kawazu, S.; Yoshida, M.; Fujii, H.; Sugi, Y. Organic–silicate hybrid catalysts based on various defined structures for Knoevenagel condensation. *Microporous Mesoporous Mater.* **2004**, *70*, 135–149. [[CrossRef](#)]
39. Macquarrie, D.J.; Jackson, D.B. Aminopropylated MCMs as base catalysts: A comparison with aminopropylated silica. *Chem. Commun.* **1997**, 1781–1782. [[CrossRef](#)]